# Accepted Manuscript

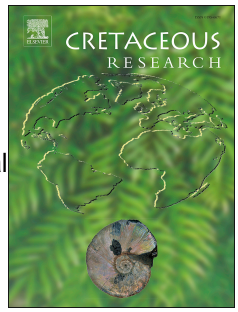


The first non-aristonectine elasmosaurid (Sauropterygia; Plesiosauria) cranial material from Antarctica: New data on the evolution of the elasmosaurid basicranium and palate

José P. O'Gorman, Rodolfo A. Coria, Marcelo Reguero, Sergio Santillana, Thomas Mörs, Magalí Cárdenas

PII: S0195-6671(17)30509-8

DOI: 10.1016/j.cretres.2018.03.013

Reference: YCRES 3833

To appear in: *Cretaceous Research*

Received Date: 22 November 2017

Revised Date: 10 March 2018

Accepted Date: 15 March 2018

Please cite this article as: O'Gorman, José.P., Coria, R.A., Reguero, M., Santillana, S., Mörs, T., Cárdenas, Magalí., The first non-aristonectine elasmosaurid (Sauropterygia; Plesiosauria) cranial material from Antarctica: New data on the evolution of the elasmosaurid basicranium and palate, *Cretaceous Research* (2018), doi: 10.1016/j.cretres.2018.03.013.

This is a PDF file of an unedited manuscript that has been accepted for publication. As a service to our customers we are providing this early version of the manuscript. The manuscript will undergo copyediting, typesetting, and review of the resulting proof before it is published in its final form. Please note that during the production process errors may be discovered which could affect the content, and all legal disclaimers that apply to the journal pertain.

ACCEPTED MANUSCRIPT

# The first non-aristonectine elasmosaurid (Sauropterygia; Plesiosauria) cranial material from Antarctica : new data on the evolution of theelasmosaurid basicranium and palate

José P. O'Gorman[a, b,*], Rodolfo A., Coria[b,c], Marcelo Reguero[a,b,d], Sergio Santillana[d], Thomas Mörs[e], Magalí Cárdenas.[f]

[a]División Paleontología Vertebrados, Museo de La Plata, Universidad Nacional de La Plata, Paseo del Bosque s/n., B1900FWA, La Plata, Argentina. *joseogorman@fcnym.unlp.edu.ar; regui@fcnym.unlp.edu.ar*

[b]CONICET, Consejo Nacional de Investigaciones Científicas y Técnicas, Argentina;

[c]Museo Carmen Funes, Av. Córdoba 55 (8318), Plaza Huincul, Neuquén, Argentina. *rcoria@unrn.edu.ar*

[d]Instituto Antártico Argentino, 25 de Mayo 1143, B1650HMK San Martín, Buenos Aires, Argentina. *ssantillana@dna.gov.ar*

[e]Department of Palaeobiology, Swedish Museum of Natural History, P.O. Box 50007, SE-104 05 Stockholm, Sweden. *thomas.moers@nrm.se*

[f]Instituto de Investigaciones en Paleobiología y Geología, Universidad Nacional de Río Negro, Av. Roca 1242 (8332), Gral. Roca, Río Negro Province, Argentina. *mcardenas@unrn.edu.ar*



*Corresponding author: O'Gorman J.P.

ABSTRACT— Elasmosaurids are a monophyletic group of cosmopolitan plesiosaurs with extremely long necks. Although abundant elasmosaurid material has been collected

from the Upper Cretaceous of Antarctica, skull material is extremely rare. Here, new elasmosaurid cranial material from the lower Maastrichtian levels of the Cape Lamb Member (Snow Hill Island Formation) on Vega Island, Antarctica is described. The studied specimen (MLP 15-I-7-6) is a non-aristonectine elasmosaurid but shows a palate morphology characterized by the absence of a posterior interpterygoid symphysis and a posterior plate-like extension of the pterygoids, features previously associated with the aristonectine palatal structure. The specimen MLP 15-I-7-6 thus provides an indication that these palatal features are also present in non-aristonectine Weddellian elasmosaurids, and makes available additional evidence of the close phylogenetical relationship between the aristonectines and some Weddellian non-aristonectine elasmosaurids.

## 1. Introduction

Elasmosaurids are a monophyletic group of plesiosaurs with extremely long necks. The biochron of this clade extends from the Early Cretaceous up to the Maastrichtian/Danian boundary (Ketchum and Benson, 2010, 2011; Benson and Druckenmiller, 2014). With a cosmopolitan distribution, it is one of the most frequently recorded groups of marine reptiles in the Late Cretaceous (Welles, 1962; Brown, 1981; Carpenter, 1999).

Remains of Antarctic Cretaceous elasmosaurids comprise tens of specimens spanning between the lower Campanian and the K/T limit (O'Gorman, 2012). With the remarkable exception of the holotype of *Morturneria seymouriensis*, the Antarctic plesiosaur specimens collected so far have not preserved any informative cranial

material (Chatterjee and Small, 1989; Gasparini et al., 2003; Martin et al., 2007; O'Gorman et al., 2012).

During the 2015 Antarctic fieldwork season in the outcrops of the Cape Lamb Member of the Snow Hill Island Formation on Vega Island (Fig.1A-C), the authors collected a new elasmosaurid specimen (MLP 15-I-7-6), that preserved an incomplete skull represented by the basicranium and portion of the palate, associated with an incomplete postcranium (Coria et al., 2015). In this contribution, we describe this specimen and provide new information about the basicranial and palatal anatomy of elasmosaurids.

*Institutional Abbreviations***.** CD, Chordata collection, National Paleontological Collection, GNS Science, Lower Hutt, New Zealand; **CM**, Canterbury Museum, Christchurch, New Zealand; **DM**, Museum of New Zealand Te Papa Tongarewa, Wellington, New Zealand; **MLP**, Museo de la Plata, Buenos Aires Province, Argentina; **MML PV**, Museo Municipal de Lamarque, Río Negro Province, Argentina;; **OU**, Otago Museum, Dunedin, New Zealand; **SGO.PV.**, Área Paleontología, Museo Nacional de Historia Natural, Santiago, Chile; **UCMP**, University of California Museum of Paleontology, California, USA; **SMNS**, Staatliches Museum fur Naturkunde, Stuttgart, Germany; **SMPSMU**, Shuler Museum of Paleontology, Southern Methodist University, Dallas, Texas, U.S.A.

*Anatomical Abbreviations*. **atc**, atlantal cup; **atrf**, atlas rib facet; **bo**, basioccipital; **bot**, basioccipital tuberosity; **bps**, basiparasphenoid; **cf**, carotid foramina; **ct**, *crista trabecularis* ; **ds**, *dorsum sellae*; **epi**, epipterygoid; **exo**, exoccipital; **lk**, lateral keel; **oc**, occipital condyle; **pa**, parapophysis; **pf**, pedicellar facet; **piv**, posterior interpterygoid vacuity; **pk**, parasphenoid keel; **plp**, posterior plate-like extension of pterygoid; **pop**, paraoccipital process; **pt**, pterygoid; **qpp**, quadrate pterygoid process; **q**, quadrate; **sq**,

squamosal; **st**, *sella turcica*; **vf**, ventral foramen; **vn**, ventral notch; **VI**, foramen for VI cranial nerve.

## 2. Geological Setting

The specimen MLP 15-I-7-6 was collected from the eastern side of Cape Lamb, on the southern shore of Vega Island, in levels corresponding to the middle part of the Cape Lamb Member of the Snow Hill Island Formation (Fig. 1), Marambio Group (Olivero, 2012). At Vega Island, these levels are represented by a coarsening upward column about 217 m thick, comprising levels of highly fossiliferous, bioturbated sandy mudstones and muddy sandstones and medium grained cross-bedded sparsely fossiliferous sandstones (Marenssi et al., 2001). This succession of sediments was deposited in a shallow environment characterized by basalmost offshore mudstones, and very fine-grained silty sandstones that pass gradationally upwards into proximal, nearshore marine, clean sandstone beds (Fig. 2; Pirrie et al., 1991; Olivero et al., 1992, 2008; Marenssi et al., 2001). The Cape Lamb Member transitionally overlies the Herbert Sound Member of the Snow Hill Island Formation and it is separated by an unconformity from the overlying Sandwich Bluff Member of the López de Bertodano Formation (Marenssi et al., 2001; Crame et al., 2004; Olivero, 2012).

The fossil fauna recognized from this member includes ammonoids genera *Gunnarites*, *Diplomoceras*, and *Jacobites* the nautiloid *Eutrephoceras*, the bivalves *Pinna* and *Lahillia*, annelids and decapods such as *Hoploparia* (Pirrie et al., 1991; Olivero et al., 1992), plesiosaurs (Martin et al., 2007; O'Gorman et al., 2012, 2015) and dinosaurs (Hooker et al., 1991; Coria et al., 2015; Rozadilla et al., 2016). Based on the ammonite fauna, Olivero (2012) placed the Snow Hill Island Formation within the

upper Campanian–lower Maastrichtian NG Sequence. The specimen MLP 15-I-7-6 comes from the Ammonite Assemblange 10 *sensu* Olivero and Medina (2000) and Olivero (2012), and is early Maastrichtian in age (Olivero and Medina, 2000; Crame et al., 2004; Olivero, 2012).

## 3. Methods

The fossil was prepared using Micro Jack and ME 9100 jackhammers. Linear measurements were taken using a digital caliper. The indices considered are those proposed by Welles (1952), which take into account the length (L), the height (H)-length centrum ratio (HI = 100 * H / L), and the breadth (B)-length centrum ratio (BI = 100 * B / L). Also, the breadth-height centrum ratio (BHI = 100 * B / H) was considered. Both breadth and height were measured on the posterior articular face. Also, the degree of vertebral elongation (Vertebral Length Index, Brown, 1981) is used (VLI = L / (0.5 * (H + B))).

In ordet to describe the basisphenoid anatomy the following therms are used. The *sella turcica* is that part of the basisphenoid that sustains the hypophysis (pituitary). The *sella turcica* contains a central recess, bounded laterally by the *crista trabecularis* and posteriorly by the *dorsum sellae*, forming a recess called “pituitary fossa” (Edinguer, 1942). Following Zverkov et al. (2017) the size of the *sella turcica* is represented as the area of an ellipse in which the length and width of the *sella turcica* are considered as major and minor axes. In order to quantify the shape and relative size of the *sella turcica,* the ratios *sella turcica* length /*sella turcica* width; 100* *sella turcica* length/basicranium length and 100*(*sella turcica* surface)$^{1/2}$/basicranial length were considered.

The ontogenetic developmental categories proposed by Brown (1981), based on the fusion of the neural arch to the vertebral centrum, were considered to to differentiate the 'adult' from the 'juvenile' growth stages.

## 4, Systematic Paleontology

Sauropterygia Owen, 1860

Plesiosauria de Blainville, 1835

Plesiosauroidea Welles, 1943

Elasmosauridae Cope, 1869

Weddellonectia O'Gorman and Coria, 2017

Weddellonectia indet.

Fig. 3-7

*Material*. MLP 15-I-7-6, partial skull comprising caudal half of pterygoids, basisphenoid, basioccipital, squamosal, exoccipital-opisthotic (Figs 3, 4); cervical, dorsal, sacral and caudal centra; cervical and dorsal ribs, partially preserved coracoid, two partially preserved propodials (Figs. 5, 6).

*Locality and Horizon*. Cape Lamb, Vega Island, Antarctic Peninsula, James Ross Archipelago; Cape Lamb Member of the Snow Hill Island Formation. Assemblage 10 of Olivero and Medina (2000), lower Maastrichtian.

## 5. Description

### *5.1. General Features*

The specimen MLP 15-I-7-6 was collected almost disarticulated over a distance of six meters. Most of the disarticulation was produced by recent solifluction weathering.

Some sectors show articulated centra, indicating that the original condition was sub-articulated (Fig. 6F, I, L).

*5.2. Skull*

The preserved sector of the skull comprises part of the posteroventral zone of the cranium, which encompasses basioccipital, basiparasphenoid (basisphenoid + parasphenoid) and exoccipital-opisthotic, posterior part of the pterygoids and squamosal (Figs 3A, B). The basiparasphenoid and pterygoids maintain their relative natural position but the basioccipital was found caudally displaced and rotated, suggesting it was not solidly fused. This condition could be attributed to the juvenile condition of the specimen. However, the absence of complete synostotic articulation between these elements has been recorded in adult elasmosaurids such as the holotype of *Libonectes morgani* and *Tuarangisaurus keyesi* (Carpenter, 1997; O'Gorman et al., 2017).

*Squamosal*. Only the caudal part of the left squamosal is preserved. It shows two lateral projections separated by an unossified area. The posterior margin bears an inflexion and a longitudinal sulcus on its dorsalmost part (Fig. 5I, J).

*Pterygoid*. The pterygoids are represented only by the caudal halves of both elements (Fig. 4). Each pterygoid delimits cranially and laterally the cultriform process of the basiparasphenoid, although no suture is visible (Fig. 4). Caudally, the pterygoids form the lateral limits of the posterior interpterygoid vacuity (piv hereafter). Caudally to the piv, the pterygoids articulate medially with the basioccipital through a medially directed small lip. They do not meet in the midline and no posterior interpterygoid symphysis is present (Fig. 4). Each pterygoid forms a plate located laterally to the piv. These plates are divided into a relatively flat, medially located area and a strongly latero-ventrally inflected zone that projects caudally. The caudal projection of pterygoids forms a posterior plate-like expansion almost at the level of the tip of the

occipital condyle in which the ventral surface become progressively medially oriented (Fig. 4). The presence of this pterygoid plate-like expansion has been observed only among aristonectine elasmosaurids. However, the condition recorded in *Aristonectes quiriquinensis*, *Kaiwhekea katiki* and *Alexandronectes zealandiensis* shows differences as the ptyerygoid posterior extension extends far posterior the occipital condyle (Otero et al., 2016).

*Epipterygoid*. Only the left epipterygoid is preserved (Fig. 3, 5A). It is a medio-laterally compressed plate with a rounded end located laterally to the *sella turcica* (Fig. 5A).

*Basioccipital*. The basioccipital forms the entire occipital condyle, which is 17.2 mm wide and 14.7 mm high (Fig. 5C-G). The condyle is strongly convex and does not show a well-defined neck. The basioccipital tuberosities project laterally and bear distally a concave surface facing antero-laterally. The dorsal surface is almost flat with two poorly defined exoccipital facets. The basioccipital body tapers cranially and its anterior end is elliptical.

*Basiparasphenoid complex*. The parasphenoid and basisphenoid are completely fused constituting a basiparasphenoid complex. The parasphenoid contributes to the complex with the ventral area of it, forming a sharp ventral keel and a ventral projection that contacts with the basioccipital (Fig. 34). In dorsal view, the lateral margins of the basisphenoid are concave. The anterior margin, which forms the *dorsum sellae*, is also strongly concave, forming an open "U" shaped notch, limited by two anterolateral rami (Fig. 4). The clinoid processes are absent. On the dorsal surface of the basisphenoid no facets for the prootic or ventral margin of *fenestra ovalis* are observed. The basipterygoid process is lateroventrally directed. The floor of the *sella turcica* is a concave area that ends cranially in a marked V-shaped notch. The *crista trabecularis* is

a convex area but not as marked as in *Tuarangisaurus keyesi* and *Libonectes morgani* (O'Gorman et al., 2017; Serratos et al., 2017: fig. S5). The anterior exit for the VI cranial nerve is located laterally to the internal carotid foramen, in a deep caudal excavation of the *sella turcica*, (Fig. 5A, B).

*Exocipital-opistootic.* The left exoccipital and opisthotic are completely fused. The paraoccipital process is thin and shows no expanded end (Fig. 5H).

*5.3. Axial Skeleton* The axial skeleton recovered is represented mostly by vertebral centra without neural arches or ribs fused. Only a few fragments of girdles and limb elements are preserved.

*Cervical region*. There are twenty-nine recovered cervical vertebrae, including the atlas and axis. The atlas-axis complex lacks the neural arch and the atlas hypocentrum (Fig. 6A-E). The dorsal surface shows the pedicellar bases of the atlas pedicels and the pedicellar facets for the axial neural arch (Fig. 6B). The ventral surface bears a ventral keel that is not complete because of the lack of the atlas hypocentrum (Fig. 6D). Posterior to the ventral keel, there are two ventral foramina. The posterior articular face is rectangular in shape. The parapophysis for the axial rib is formed by the contribution of both atlas and axis centra (Fig. 6C).

Almost all of the post atlas-axis centra are longer than high, and broader than long (Table I). In dorsal view, the pedicellar facets of the anterior centra are cranio-caudally elongated (Fig. 6M). On the floor of the neural canal there are two foramina (Fig. 6M). The lateral faces of some vertebrae show a lateral keel (Fig. 6I). The articular faces show a ventral notch (Fig. 6G, H). In ventral view, a pair of ventral foramina are visible (Fig. 6F, J, N). The prezygapophyses and postzygapophyses are confluent in the midline and strongly medially inclined.

*Pectoral region*. Only fragments of the pectoral region are preserved. However, they are too incomplete for a detailed description.

*Dorsal region*. Eight dorsal centra are well preserved. The articular faces have a circular outline. The lateral sides are cranio-caudally concave. The pedicellar facets are cranio-caudally elongate and concave. The dorsal centra are pierced by two to three ventral foramina located on the ventral to ventro-lateral surface of the centra (Fig. 6O-R).

*Sacral region*. Only the last sacral centrum is preserved. It is wider than high, and higher than long. On the ventral surface there is one ventral foramen (Fig. 7A-C).

*Caudal region*. Only the first caudal vertebra and another from the middle part of the tail are preserved. They are broader than high, and higher than long. The first caudal vertebrae shows no haemal arch, whereas the other preserved centrum bear slightly developed haemal facets (Fig. 7F). Both centra show a single ventral foramen (Fig. 7C, F).

*5.4. Appendicular Skeleton*

*Pectoral girdle*. Only fragments of the girdles are preserved, including part of the coracoids that preserved a mid ventral process.

*Propodials*. Two propodial elements are preserved (Fig. 7G-M), although their certain identification is not possible. Towards the proximal ends, there is a partially preserved muscle scar that allows a determination of the ventral margin of the bones. On the mid shaft, there are few and relatively large foramina (Fig. 7H, J). Both elements bear a slightly convex and rugose area almost on the anterior margin of the ventral surface. The pattern of fracture in the propodial permits a view of the clear separation between perichondral and endochondral ossification (Fig. 7I, M).

## 6. Discussion

### *6.1. Ontogenetic stage and systematic affinities of MLP 15-I-7-6*

The juvenile ontogenic stage of MLP 15-I-7-6 is suggested by the following features: 1) the neural arches are not fused with the vertebral centra; 2) the cervical and caudal ribs are not fused with their corresponding vertebral centra, and 3) the way in which the propodials are broken indicates that the limit between the perichondral and endochondral bone was not affected by secondary remodeling (Brown, 1981; O'Gorman et al., 2017).

The specimen MLP 15-I-7-6 shows unquestionable elasmosaurid affinities based on the dumbbell shape of the articular faces on cervical centra (Benson and Druckenmiller, 2014; Otero et al., 2014; Otero, 2016; O'Gorman, 2016). In turn, the presence of flat articular faces on cervical centra, cervical centra with zygapophyses fused in the midline, and zygapophyses narrower than the centra, are features shared by all elasmosaurids and independently acquired in other plesiosaurs such as *Muraenosaurus leedsi* (Benson and Druckenmiller, 2014).

The specimen MLP 15-I-7-6 is here considered a non-aristonectine elasmosaurid because the values of the HI and BI indexes of the posterior cervical centra differ from those of juvenile aristonectines (O'Gorman et al., 2013, 2014a, b, Fig. 8) but also differd from the tipical proportions of adult non-aristonectines (Fig. 9). In addition, the posterior extension of the pterygoid of MLP 15-I-7-6 is shorter than previously recorded among aristonectines (Otero et al., 2016).

However, the comparison of MLP 15-I-7-6 with the non-aristonectine taxa from the Weddellian Biogeographic Province (hereafter WBP): *Tuarangisaurus keyesi* Wiffen and Moisley, 1986, *Kawanectes lafquenianum* (Gasparini and Goñi) O'Gorman,

2016, and *Vegasaurus molyi* O'Gorman, Salgado, Olivero, Marenssi, 2015 is limited mainly for two reasons. First, the juvenile ontogenic stage of MLP 15-I-7-6 contrasts with the adult condition of the holotype specimens of the above-mentioned species, and second, the virtually total lack of postcranial material in the holotype of *Tuarangisaurus keyesi* (NPC CD 425 and NPC CD 426), and the unknown skulls of both *Kawanectes lafquenianum* and *Vegasaurus molyi*.

The available skull material of *Tuarangisaurus keyesi* overlaps with almost all of the elements present in MLP 15-I-7-6 with the exception of the occipital condyle. The pterygoids of *T. keyesi* and MLP 15-I-7-6 show almost no differences. Even both show a triradiate cross section of pterygoid at the level of the basiparasphenoid and basioccipital suture (Fig. 10C). However, as this feature is also present in other elasmosaurids such as *Libonectes morgani* (see Carpenter, 1997:fig.5A)and therefore this feature seems to be not diagnostic at genus level. The absence of posterior pterygoid symphysis in MLP 15-I-7-6 cannot be contrasted with *T. keyesi* due to the deficient preservation in that area. The basisphenoid of *T. keyesi* shows a small anterior exit for the VI cranial nerve on the anterior surface of the *dorsum sellae*, whereas in MLP 15-I-7-6, the VI cranial nerve exits on the back of the *sella turcica* through two large foramina. In addition, the *sella turcica* of MLP 15-I-7-6 ends in a marked notch, which is absent in *T. keyesi* (O'Gorman et al., 2017). Recently the specimen CM Zfr 115 was referred to *Tuaragisaurus* sp. and therefore it should be compared with MLP 15-I-7-6. The dorsal surfaces of the basioccipitals of MLP 15-I-7-6 and CM Zfr 115 share the relatively wide separation between the exoccipital facets that differ from the observed in *Alexandronectes zealandiensis*. The cervical centra of MLP 15-I-7-6 are less elongated that the ones of CM Zfr 115, however this could be related with the

different growth stage as CM Zfr 115 is adult whereas MLP 15-I-7-6 belong to a juvenile individual (Fig. 9).

With regard to the postcranial anatomy, cervical vertebrae bearing lateral keels are frequently present among elasmosaurids but they are absent in *Aristonectes parvidens*; *Kaiwhekea katiki* and *Nakonanectes bradti* (Cruckshank and Fordyce, 2002; O'Gorman, 2016; Serratos et al., 2017). The proportions of the cervical centra of elasmosaurids (Fig. 9) vary during the ontogeny as the relative length of vertebral centra changes. Such changes generate an increment of VLI, and a decline of BI and HI values (O'Keefe and Hiller, 2006). Thus, MLP 15-I-7-6 is more similar to *Vegasaurus molyi* than to any other Weddellian elasmosaurids and part of the differences could be related to ontogenetic variation. However, as the general proportions of the vertebral centra should be taken with caution as diagnostic feature, the specimen here is regarded as Weddellonectia indet. The caudal vertebrae of MLP 15-I-7-6 show parapophyses that are not as laterally projected as in *Kawanectes lafquenianum* (O'Gorman, 2016).

*6.2. Palate Structure*

The palate area of MLP 15-I-7-6 (Fig. 10C) shows no posterior interpterygoid symphysis, and pterygoids extended until the level of the occipital condyle unlike the condition present in the non-aristonectine elasmosaurids *Libonectes morgani* and *Callawayasaurus colombiensis* (see Fig. 10A, B) where the pterygoid quadrate ramus shows a stick like morphology. In contrast, the posterior plate-like expansion of the pterygoid is similar to the condition present in the aristonectines *Alexandronectes zealandiensis* and *Aristonectes quiriquinensis* (Otero et al., 2016: fig. 9D; Fig 10D, Fig. 11). However, the plate-like posterior expansion of the pterygoids in those taxa is extended far posterior the occipital condyle .

Although the juvenile condition of MLP 15-I-7-6 certainly affects the degree of ossification in several skull elements, the pterygoids show well-defined sutures. Thus, it is possible to expect no major ontogenetic variation between the specimen MLP 15-I-7-6 and its adult stage. Consequently, the presence of a posterior plate-like extension of the pterygoid (although different in its posterior extension) in the specimen MLP 15-I-7-6 indicates that it can be considered a feature present in both aristonectine and non-aristonectine elasmosaurids . This raises the question about the aristonectine affinities of *Alexandronectes*, which were based on the posterior plate-like extension of the pterygoid (Otero et al., 2016). However as has been stated the posterior extension is less developed in MLP 15-I-7-6 and therefore it could represent an intermediate stage in the change between the pterygoid morphology of aristonectine and non-aristonectine elasmosurids. Additionally, the posterior interpterygoid symphysis could be also absent in *T. keyesi,* although there is no certainty about this point, due to the poor preservation of this area in the *T. keyesi* holotype (O'Gorman et al., 2017, Fig. 10E) and the CM Zfr 115, referred to *Tuarangisaurus* sp. (Hiller et al., 2017)..

*6.3. Braincase comparison*

*Basioccipital*. The dorsal surface of the basioccipital of MLP 15-I-7-6 is anteriorly inclined (about 30°) as in other elasmosaurids such as *Callawayasaurus colombiensis* (J.P.O'G pers. obs. UCPM 38349), *T. keyesi* and *A. zealandiensis* (Otero et al., 2016; O'Gorman et al. 2017).

The specimen MLP 15-I-7-6 shows an unossified area between the basioccipital and the basiparasphenoid like in adult specimens of *Libonectes morgani* and *Tuarangisaurus keyesi* (Carpenter, 1999; O'Gorman et al., 2017). In other plesiosaurs, like the polycotylid *Edgarosaurus muddy*, the basioccipital and basiparasphenoid remain unfused (Druckenmiller, 2002). On the other hand, a similar although larger

unossified zone is recorded for *Pliosaurus almanzaensis* (O'Gorman et al., 2018). The occipital condyle of MLP 15-I-7-6 lacks a well-defined neck, unlike *Libonectes morgani*, *Callawayasaurus colombiensis* and *Alexandronectes zealandiensis* and the polycotylid *Trinacromerum bentonianum* (Carpenter, 1997; O'Keefe, 2004; Otero et al., 2016).

*Basiparasphenoid*. The Basiparasphenoid embraces ventrally the basioccipital condyle through a ventral projection. This condition has been observed in *Tuarangisaurus keyesi* (adult specimen) and in the pliosaurid *Pliosaurus almanzaensis,* although in the latter, a pair of ventrolateral projections is also present (O'Gorman et al., 2018).

The anterior limit of the floor of the *sella turcica* shows a V-shaped notch. This notch is also present in the Elasmosauridae indet SGU 251/1 from the lower Campanian of Saratov Province, Russia (Zverkov et al., 2017). This feature is absent in *Dolichorhynchops* sp., *Brancasaurus brancai*, *Edgarosaurus muddi* (Sato et al., 2011; Druckenmiller, 2002; Wegner, 1914) and *Tricleidus seeleyi* (Andrews, 1910 fig. 73), but is present as a small notch in *Plesiopterys wildi* (O'Keefe, 2004). Therefore, the anterior well developed notch seems to be a feature only observed in elasmosaurids.

The specimen MLP 15-I-7-6 shows a keeled parasphenoid, which is a feature present in *Tuarangisaurus keyesi*, *Callawayasaurus colombiensis*, *Libonectes morgani* among other elasmosaurids (Benson and Druckenmiller, 2014; O'Gorman et al., 2017). A similar keeled parasphenoid is also present in the polycotylids *Edgarosaurus muddi*, *Nichollssaura borealis*, and *Pahasapasaurus haasi* (Druckenmiller, 2002; Schumacher, 2007; Sato et al., 2011), but differs from what is observed in *Trinacromerum bentonianum*, *Dolychorhynchops osborni*, *D. bonneri* and *D. herschelensis*, which bear a keel with bean-shaped cross section (Sato et al., 2011).

The internal carotid foramen of MLP 15-I-7-6 could pierce the caudal limit of the pituitary fossa as in the elasmosaurids *A. zealandiensis*, *T. keyesi* and *L. morgani* and is unlike the polycotylid *Dolychorynchops* (floor of pituitary fossa, Sato et al., 2011) and the pliosaurid *Thalassiodracon hawkinsi* (between the back and floor of the pituitary fossa, Benson et al., 2013; Benson and Druckenmiller, 2014). The internal carotids exiting in the pituitary fossa are paired in MLP 15-I-7-6 as in *T. keyesi*, but there is only a single medial foramen in *A. zealandiensis* and *L. morgani* (Serratos et al., fig. S5; Otero et al., 2016). In *L. morgani* both conditions are observed: as a single medial foramen as recorded in the SMU SMP 69120 (holotype), or as two separate foramina in the referred specimen SMNK-PAL 3978 (Serratos et al., 2017: fig. S5; Allemand et al., 2017).

The foramen for the exit of the VI cranial nerve on the back of the pituitary fossa in MLP 15-I-7-6 differs from *A. zealandiensis*, *L. morgani* and *T. keyesi*, in which the nerve exits laterally to the pituitary fossa through the anterior limit of the lateral process of the *dorsum sellae* (Otero et al., 2016; O'Gorman et al., 2017; Serratos et al., 2017: fig. S5). The foramen for the VI cranial is as large as each carotid foramen in MLP 15-I-7-6 contrasting with the relatively small opening, smaller than the internal carotid foramen of *A. zealandiensis* and *T. keyesi*. (O'Gorman et al., 2017; Otero et al 2016). The case of *L. morgani* is complex because the foramen for the VI cranial nerve is as large as or larger than the confluence of the carotid foramina in the holotype specimen (SMU SMP 69120), but is clearly smaller in the referred specimen SMNK-PAL 3978 (Serratos et al., 2017: fig. S5; Allemand et al., 2017 fig. 5C). The specimen SGU 251/1 (Zverkov et al., 2017) shows a condition that resembles that of SMU SMP 69120 (holotype).

The paraoccipital process of MLP 15-I-7-6 is long and not distally expanded as in *Tuarangisaurus keyesi* and *Aristonectines quiriquinensis* (Otero et al., 2014; O'Gorman et al., 2017). On the other hand, a paraoccipital process with expanded distal end is present in *Libonectes morgani*, *Callawayasaurus colombiensis* and *Alexandronectes zealandiensis* (Welles, 1962; Carpenter, 1997; Otero et al., 2016).

*6.4. Sella turcica* (*pituitary fossa*) *proportions*

Recent works on the proportions of the braincases of Plesiosauria show an unexpected diversity. Indeed, Sato et al. (2011) comment that the ratio between the length of the pituitary fossa and the basicranium floor varies between 1/6 and 1/3. Recently, Sverko et al. (2017) quantified the size of the pituitary fossa and described its correlation with the complete basicranial length. Figure 12F shows the plot of ratio values of *sella turcica* length/basicranial length vs *sella turcica* length/*sella turcica* width. The figure 12F shows two groups of elasmosaurids: one group formed by *Libonectes morgani* and Elasmosauridae indet (SGU 251/1); the other group formed by the other considered elasmosaurids *T. keyesi*; *Ar. quiriquinensis* and MLP 15-I-7-6. Figure 12G shows a proxy of the ratio between the relative surfaces occupied by the *sella turcica* (see Material and Methods). The specimen MLP 15-I-7-6 shows the higher values along with *Aristonectes quiriquinensis*. Although the taxon sampling is limited, the available data both comparisons (Fig. 12 F, G)seems to indicate similarities between the MLP 15-I-7-6 and the aristonectine Weddellonectia. These similarities could be related to phylogenetical affinities within Weddellonectia, or they could be related to the juvenile condition of the MLP 15-I-7-6, and the pedomorphic condition present in adult aristonectines (O'Gorman et al., 2014a; Araujo et al., 2015).

## 7. Conclusions

The specimen MLP 15-I-7-6 is a juvenile non-aristonectine elasmosaurid plesiosaur. The palate shows one feature previously recorded only in *Aristonectes quiriquinensis* and *Alexandronectes zealandiensis*: the absence of a posterior interpterygoid symphysis. Additionally a posterior plate like extension of the pterygoid of MLP 15-I-7-6 is similar to the one recorded in aristonetines although less posterior extended. This indicates that the changes in the palatal morphology started previously to the development of other aristonectine features.

**Acknowledgments**

This contribution would not have been possible without logistical support from the Instituto Antártico Argentino and the Fuerza Aérea Argentina (Dotación 48° of Base Marambio) and M. Reguero (PICTO 2010-0093). K. Kamra assisted with language editing. This research was supported by projects UNLP N 607, PICT 2015-0678, VR 2009-4447. The authors thank E. Montes (Museo Carmen Funes, Plaza Huincul, Neuquén Province, Argentina) and F. Solari Orellana (MLP) for the lab-preparation of MLP 15-I-7-6 and P. Druckenmiller (University of Alaska Museum) for providing photos of *L. morgani* and R. Otero (Laboratorio de Ontogenia y Filogenia, Universidad de Chile) for assistance in extension of measures. The authors also thank R. Otero and N. Hiller (Canterbury Museum) for their review comments that improved this contribution, and L. Chornogubsky and G. López for their assistance during the fieldwork.

## References

Andrews, C.W., 1910. A catalogue of the marine reptiles of the Oxford Clay, Part I. British Museum (Natural History), London, England.

Allemand, R., Bardet, N., Houssaye, A., Vincent, P., 2017. Virtual reexamination of a plesiosaurian specimen (Reptilia, Plesiosauria) from the Late Cretaceous (Turonian) of Goulmima, Morocco, using computed tomography. Journal of Vertebrate Paleontology 37, e1325894.

Araújo, R., Polcyn, M.J., Lindgren, J., Jacobs, L.L., Schulp, A.S., Mateus, O., Goncalves, O., Morais, M-L., 2015. New aristonectine elasmosaurid plesiosaur specimens from the Early Maastrichtian of Angola and comments on paedomorphism in plesiosaurs. Netherlands Journal of Geosciences 94, 93-108.

Blainville de, H.M.D., 1835. Description de quelques espèces de reptiles de la Californie, précédée de l'analyse d'un systéme générale d'Erpetologie et d'Amphibiologie. Nouvelles Annales du Muséum d'Historie Naturelle, Paris 4, 233-296.

Benson, R.B., Bates, K.T., Johnson, M.R., Withers, P.J., 2011. Cranial anatomy of *Thalassiodracon hawkinsii* (Reptilia, Plesiosauria) from the Early Jurassic of Somerset, United Kingdom. Journal of Vertebrate Paleontology 31, 562-574.

Benson, R.B., Druckenmiller, P.S., 2014. Faunal turnover of marine tetrapods during the Jurassic–Cretaceous transition. Biological Reviews 89, 1-23.

Brown, D.S., 1981. The English Upper Jurassic Plesiosauroidea (Reptilia) and a review of the phylogeny and classification of the Plesiosauroidea. Bulletin of British Museum of Natural History, (Geology) 35, 253-347.

Carpenter, K., 1997. Comparative cranial anatomy of two North American Cretaceous plesiosaurs. In: Callaway, J.M., Nicholls, E.L. (Eds.). Ancient marine reptiles. Academic Press, San Diego, 191-216.

Carpenter, K., 1999. Revision of North American elasmosaurids from the Cretaceous of the Western Interior. Paludicola 2, 148-173.

Chatterjee, S., Small, B.J., 1989. New plesiosaur from the Upper Cretaceous of Antarctica. Special Publications of the Geological Society 47, 197-215.

Cope, E.D., 1869. Synopsis of the extinct Batrachia, Reptilia and Aves of North America. Transaction of the American Philosophical Society (new series) 14, 1-252.

Coria, R.A., O'Gorman, J.P., Cárdenas, M., Gouiric-Cavalli, S., Mörs, T., Chornogubsky, L., López, G., 2015. Late Cretaceous vertebrates from Isla Vega, Antarctica: Reports from the 2015 fieldwork. Ameghiniana 52, Supp.: 12-13.

Crame, J.A., Francis, J.E., Cantrill, D.J., Pirrie, D., 2004. Maastrichtian stratigraphy of Antarctica. Cretaceous Research 25, 411-423.

Cruickshank, A.R., Fordyce, R.E., 2002. A new marine reptile (Sauropterygia) from New Zealand: further evidence for a Late Cretaceous austral radiation of cryptoclidid plesiosaurs. Palaeontology 45, 557-575.

Druckenmiller, P.S., 2002. Osteology of a new plesiosaur from the Lower Cretaceous (Albian) Thermopolis Shale of Montana. Journal of Vertebrate Paleontology 22, 29-42.

Edinger, T., 1942. The pituitary body in giant animals fossil and living: a survey and a suggestion. The Quarterly Review of Biology 17, 31-45.

Gasparini, Z., Martin, J.E., Fernández, M., 2003. The elasmosaurid plesiosaur *Aristonectes* Cabrera from the Latest Cretaceous of South America and Antarctica. Journal of Vertebrate Paleontology 23, 104-115.

Hooker, J., Milner, A., Sequeira, S., 1991. An ornithopod dinosaur from the Late Cretaceous of West Antarctica. Antarctic Science 3, 331-332. doi:10.1017/S0954102091000391

Ketchum, H.F., Benson R.B.J., 2010. Global interrelationships of Plesiosauria (Reptilia, Sauropterygia) and the pivotal role of taxon sampling in determining the outcome of phylogenetic analyses. Biological Reviews 85, 361-392.

Ketchum, H.F., Benson R.B.J., 2011. A new pliosaurid (Sauropterygia, Plesiosauria) from the Oxford Clay Formation (Middle Jurassic, Callovian) of England: evidence for a gracile, longirostrine grade of Early–Middle Jurassic pliosaurids. Special Papers in Palaeontology 86, 109-129.

Marenssi, S.A., Salani F.M., Santillana S.N., 2001. Geología del Cabo Lamb, Isla Vega, Península Antártica. Instituto Antártico Argentino. Contribución 530, 1-43.

Martin, J. E., Sawyer J.F,. Reguero M., Case J.A., 2007. Occurrence of a young elasmosaurid plesiosaur skeleton from the Late Cretaceous (Maastrichtian) of Antarctica. Online Proceedings of the 10th International Symposium on Antarctic Earth Sciences. Open Report 2007-104, Short Research Paper 066, 4 pp.

O'Gorman, J. P., 2012. The oldest elasmosaur (Sauropterygia, Plesiosauria) from Antarctica, Santa Marta Formation (Coniacian?Santonian–lower Campanian) and Snow Hill Island Formation (upper Campanian–lower Maastrichtian), James Ross Island. Polar Research 31, 1-10.

O'Gorman, J.P., 2016. A small body sized non-aristonectine elasmosaurid (Sauropterygia, Plesiosauria) from the Late Cretaceous of Patagonia with comments on the relationships of the Patagonian and Antarctic elasmosaurids. Ameghiniana 53, 245-268.

O'Gorman, J.P., Coria, R.A. 2017. A new elasmosaurid specimen from the upper Maastrichtian of Antarctica: new evidence of a monophyletic group of Weddellian elasmosaurids. Alcheringa: An Australasian Journal of Palaeontology 41, 240-249.

O'Gorman, J.P., Gasparini, Z., Spalleti, L.A. A new Pliosaurus species (Sauropterygia, Plesiosauria) from the Upper Jurassic of Patagonia: new insights on the Tithonian morphological disparity of mandibular symphyseal morphology. Journal of Paleontology. doi: 10.1017/jpa.2017.82. in press

O'Gorman, J.P., Olivero, E., Cabrera, D., 2012. Gastroliths associated with a juvenile elasmosaur (Plesiosauria, Elasmosauridae) from Snow Hill Island Formation (upper Campanian–lower Maastrichtian), Vega Island, Antarctica. Alcheringa 36, 531-541.

O'Gorman, J.P, Gasparini, Z., Salgado, L., 2013. Postcranial morphology of *Aristonectes* Cabrera, 1941 (Plesiosauria, Elasmosauridae) from the Upper Cretaceous of Patagonia and Antarctica. Antarctic Science 25, 71-82.

O'Gorman, J.P., Gasparini, Z., Salgado, L., 2014a. Reappraisal of *Tuarangisaurus*? *cabazai* (Elasmosauridae, Plesiosauria) from the upper Maastrichtian of northern Patagonia, Argentina. Cretaceous Research 47, 39-47.

O'Gorman, J.P., Otero, R.A., Hiller, N., 2014b. A new record of an aristonectine elasmosaurid (Sauropterygia, Plesiosauria) from the Upper Cretaceous of New Zealand: implications for the Mauisaurus haasti Hector, 1874 hypodigm. Alcheringa: An Australasian Journal of Palaeontology 38, 504-512.

O'Gorman, J.P., Talevi, M., Fernández, M.S. , 2017. Osteology of a perinatal aristonectine (Plesiosauria; Elasmosauridae). Antarctic Science 29, 61-72.

O'Gorman, J.P., Salgado, L., Olivero, E.B., Marenssi, S.A., 2015. *Vegasaurus molyi*, gen. et sp. nov.(Plesiosauria, Elasmosauridae), from the Cape Lamb Member (lower Maastrichtian) of the Snow Hill Island Formation, Vega Island, Antarctica, and remarks on Wedellian Elasmosauridae. Journal of Vertebrate Paleontology, 35: e931285.

O'Gorman, J.P., Otero, R.A., Hiller, N., Simes, J., Terezow, M., 2017. Redescription of *Tuarangisaurus keyesi* (Sauropterygia; Elasmosauridae), a key species from the uppermost Cretaceous of the Weddellian Province: Internal skull anatomy and phylogenetic position. Cretaceous Research 71, 118-136.

O'Keefe, F.R., 2004. Preliminary description and phylogenetic position of a new plesiosaur (Reptilia: Sauropterugia) from the Toarcian of Holsmaden, Germany. Journal of Paleontology 78, 973-988.

O'Keefe, F.R., Hiller, N., 2006. Morphologic and ontogenetic patterns in elasmosaur neck length, with comments on the taxonomic utility of neck length variables. Paludicola 5, 206-229.

Olivero, E.B., 2012. Sedimentary cycles, ammonite diversity and palaeoenvironmental changes in the Upper Cretaceous Marambio Group, Antarctica. Cretaceous Research 34, 348-366.

Olivero, E.B., Martinioni D.R., Mussel F.J., 1992. Sedimentología y bioestratigrafía del Cretácico Superior de Cabo Lamb (Isla Vega, Antártida). Implicancias sobre ciclos sedimentarios y evolución de la cuenca. In: Rinaldi C.A. (ed.), Geología de la Isla James Ross, Instituto Antártico Argentino, Buenos Aires., 125–145

Olivero, E.B., Medina F.A., 2000. Patterns of Late Cretaceous ammonite biogeography in southern high latitudes: the family Kossmaticeratidae in Antarctica. Cretaceous Research 21, 269–279.

Olivero, E.B.,. Ponce J.J., Martinioni D.R., 2008. Sedimentology and architecture of sharp-based tidal sandstones in the upper Marambio Group, Maastrichtian of Antarctica. Sedimentary Geology 210, 11-26.

Otero, R.A., 2016. Taxonomic reassessment of Hydralmosaurus as Styxosaurus: new insights on the elasmosaurid neck evolution throughout the Cretaceous. PeerJ 4, e1777.

Otero, R.A., O'Gorman, J.P., Hiller, N., O'Keefe, F.R., Fordyce, R. E., 2016. *Alexandronectes zealandiensis* gen. et sp. nov., a new aristonectine plesiosaur from the lower Maastrichtian of New Zealand. Journal of Vertebrate Paleontology, 36: e1054494.

Otero, R.A., Soto-Acuña, S., O'Keefe, F.R., O'Gorman, J.P., Stinnesbeck, W., Suárez, M.A., Rubilar-Rogers, D., Quinzio-Sinn, L.A., Salazar, C., 2014. *Aristonectes quiriquinensis* sp. nov., a new highly derived elasmosaurid from the late Maastrichtian of central Chile. Journal of Vertebrate Paleontology 34, 100-125.

Owen, R., 1860. On the orders of fossil and recent Reptilia, and their distribution in time. Reports of the British Association for the Advancement of Science 29, 153-166.

Pirrie, D., Crame, J.A., Riding, J.B., 1991. Late Cretaceous stratigraphy and sedimentology of Cape Lamb, Vega Island, Antarctica. Cretaceous Research 12, 227-258.

Rozadilla, S., Agnolin, F.L., Novas, F.E., Rolando, A.M.A., Motta, M.J., Lirio, J.M., Isasi, M.P., 2016. A new ornithopod (Dinosauria, Ornithischia) from the Upper Cretaceous of Antarctica and its palaeobiogeographical implications. Cretaceous Research 57, 311-324.

Sato, T., Wu, X.C., Tirabasso, A., Bloskie, P., 2011. Braincase of a polycotylid plesiosaur (Reptilia: Sauropterygia) from the Upper Cretaceous of Manitoba, Canada. Journal of Vertebrate Paleontology 31, 313-329.

Schumacher, B.A., 2007. A new polycotylid plesiosaur (Reptilia; Sauropterygia) from the Greenhorn Limestone (Upper Cretaceous; lower upper Cenomanian), Black Hills, South Dakota. Geological Society of America Special Papers 427, 133-146.

Serratos, D.J., Druckenmiller, P.., Benson, R. B., 2017. A new elasmosaurid (Sauropterygia, Plesiosauria) from the Bearpaw Shale (Late Cretaceous, Maastrichtian) of Montana demonstrates multiple evolutionary reductions of neck length within Elasmosauridae. *Journal of Vertebrate Paleontology*, e1278608.

Wegner, T.H., 1914. *Brancasaurus brancai* n. g. n. sp., ein Elasmosauride aus dem Wealden Westfalens. In: Festschrift für Wilhelm Branca zum 70. Geburtstage 1914. Leipzig: Borntraeger. 235-305

Welles, S.P., 1943. Elasmosaurid plesiosaurs with description of new material from California and Colorado. Memoirs of the University of California 13, 125-254.

Welles, S.P., 1952. A review of the North American Cretaceous elasmosaurs. University of California. Publications in Geological Sciences 29, 47-144.

Welles, S.P., 1962. A New species of elasmosaur from the Aptian of Colombia and a review of the Cretaceous plesiosaurs. University of California. Publications in Geological Sciences 44, 1-96.

Wiffen, J., Moisley, W.L., 1986. Late Cretaceous reptiles (Families Elasmosauridae and Pliosauridae) from the Mangahouanga Stream, North Island, New Zealand. New Zealand Journal of Geology and Geophysics 29, 205-252.

Zverkov, N. G., Averianov, A. O., Popov, E.V., 2017. Basicranium of an elasmosaurid plesiosaur from the Campanian of European Russia. Alcheringa: An Australasian Journal of Palaeontology, (in press). dx.doi.org/10.1080/03115518.2017.1302508

ACCEPTED MANUSCRIPT

FIGURE CAPTIONS

**Fig. 1. A, B** Maps of Cape Lamb, Vega Island, Antarctica. The star shows the locality where the MLP 15-I-7-6 was collected (Modifed from Marenssi et al., 2001). **C**, schematic sketch showing the recovered material shaded in grey.

**Fig. 2.** Sedimentary log showing location of the site where MLP 15-I-7-6 was collected. Other relevant vertebrates collected in the vicinity are also indicated (modified from Pirrie at al., 1991; O'Gorman et al., 2015).

**Fig. 3**. MLP 15-I-7-6, Elasmosauridae indet. Cranium in dorsal view. **A**, photo and **B**, interpretative diagram. . Scale bar = 20mm. Abbreviations: bo, basioccipital; bps, basiparasphenoid; oc, occipital condyle; epi, epypterigois; plp, posterior plate-like extension of pterygoid; pt, pterygoid; sq, squamosal; st, sella turcica. Scale bar = 20 mm.

**Fig. 4**. MLP 15-I-7-6, Elasmosauridae indet. Cranium in ventral view. **A**, photo and **B**, interpretative diagram. Scale bar = 20mm. Abbreviations: bo, basioccipital; bps, basiparasphenoid; oc, occipital condyle; piv, posterior interpterygoid vacuity; plp, posterior plate-like extension of pterygoid; pt, pterygoid; pk, parasphenoid keel; sq, squamosal. Scale bar = 20 mm.

**Fig. 5**. MLP 15-I-7-6, Elasmosauridae indet. Basisphenoid in **A**, anterior and **B**, dorsal views. **C-G** basioccipital in **C**, dorsal, **D**, ventral, **E**, posterior, **F**, right lateral views, **G**, anterior views. **H**, exoccipital-opistothic, **I-J**, left squamosal in **I**, lateral and **J**, posterior views. bot, basioccipital tuberosity; cf, carotid foramina; **ct**, *crista trabecularis*; ds, *dorsum sellae*; exo, exoccipital; oc, occipital condyle; pop, paraoccipital process; sq, squamosal; st, *sella turcica*; VI, foramen for VI cranial nerve. Scale bars = 20mm.

**Fig. 6**. MLP 15-I-7-6, Elasmosauridae indet. A-E. atlas-axis complex in **A**, anterior, **B**, dorsal, **C**, left lateral, **D**, ventral and **E**, posterior views. **F-G**, anterior cervical vertebrae

in **F**, ventral and **G**, posterior views. **H-J**, middle cervical vertebrae in **H**, anterior, **I** right lateral and **J,** ventral views. **K-N**, posterior cervical vertebrae in **K**, anterior, **L**, right lateral, **M**, dorsal and **N**, ventral views. **O-R** dorsal vertebral centrum in **O**, anterior, **P**, dorsal, **Q**, ventral and **R**, lateral views. Abbreviations: atc, atlantal cup; atrf, atlas rib facet; lk, lateral keel, pa, parapophysis; pf, pedicellar facet; vf, ventral foramen; vn, ventral notch. Scale bar = 20 mm

**Fig. 7**. MLP 15-I-7-6, Elasmosauridae indet. **A-C**, posteriormost sacral and first caudal vertebrae in **A**, dorsal, **B**, left lateral and **C**, ventral views. **D-F**, caudal vertebrae in **D**, anterior, **E**, dorsal and **F**, ventral views. **G-I** left propodium in **G**, dorsal, **H**, ventral and **I**, proximal views. **J-M**, right propodium in **J**, ventral, **K**, dorsal, **L**, proximal and **M**, distal views. Black arrows indicate limit between perichondral and edochondral ossifications. Abbreviations: pa, parapophysis; pf, pedicellar facet; vf, ventral foramen. Scale bars = 20 mm.

**Fig. 8**. Plots of HI and BI of cervical centra of MLP 15-I-7-6 and juvenile elasmosaurids (aristonectine and non-aristonectine modified from O'Gorman et al., 2013).

**Fig. 9**. Plots of HI, BI and VLI of cervical centra vs the vertebral position of several Weddellian non-aristonectine elasmosaurids (Data taken from Wiffen and Moisley, 1986; O'Keefe and Hiller, 2006; O'Gorman et al., 2015; O'Gorman, 2016).

**Fig. 10**. Palatal structure of elasmosaurids. **A**, (UCPM 125328) *Callawayasaurus colombiensis*; **B**, *Libonectes morgani* (SMUSMP 69120), **C**, Elasmosauridae indet.

MLP 15-I-7-6 and pterygois in cross section; **D**, *Alexandronectes zealandiensis* (CM Zfr 91). Diagrams of area preserved in *T. keyesi* compared with a generalised Elasmosauridae palate (e.g. *Libonectes*). Scale bars = 20 mm. Abbreviations; bas, basiparasphenoid; bo, basioccipital; cf, carotid foramen; oc, occipital condyle; piv, posterior interpterygoid vacuity; pt, pterygoid; q, quadrate; qrp, quadrate ramus of pterygoid.

**Fig. 11**. Diagram showing the different pterygoid morphologies in **A**, several non-aristonectines; **B**, non-aristonectine MLP 15-I-7-6 and **C**, Aristonectines (*Alexandronectes*, *Aristonectes*). Based on Carpenter, 1999; Otero et al., 2016 and J.P.O'G per sobs. Abbreviations; bas, basiparasphenoid; bo, basioccipital; cf, carotid foramen; oc, occipital condyle; piv, posterior interpterygoid vacuity; pt, pterygoid; q, quadrate; qrp, quadrate ramus of pterygoid.

**Fig. 12**. Schematic representation of the basisphenoid. **A**-**B**, MLP 15-I-7-6 in **A**, dorsal and **B**, anterior views. **C**-**E** other elasmosaurids in anterior view **C**, *Tuarangisaurus keyesi*; **D**, *Alexandronectes zealandiensis*; **E**, *Libonectes morgani*; **F** plots of *sella turcica* length/basicranium length vs 100**sella turcica* wide/*sella turcica* length. **G**, 100* (*sella turcica* surface)$^{1/2}$ /basicranial length.(Data taken from Sverkov et al., 2017; Otero pers comm.). cf, carotid foramina; ct, *crista trabecularis*; ds, *dorsum sellae*; st, *sella turcica*; VI, foramen for VI cranial nerve.

ACCEPTED MANUSCRIPT

Table I. Measurements and indeces of vertebral centra. L, length; H, height and B, breadth (all in mm), HI, height (H)/length (L) ratio (HI=100*H/L), BI, breadth (B)/length (L) ratio (BI=100*B/L), BHI, breadth/height ratio (BHI=100*B/H) and VLI, Vertebral Length Index [VLI=100*L/((H + B)/2)]. Approximate values in italics.

| Región | L | H | B | HI | BI | BHI | VLI |
|---|---|---|---|---|---|---|---|
| Ce | 24 | 14 | 20 | 58 | 83 | 143 | 141 |
| Ce | 19 | 19 | 26 | 100 | 137 | 137 | 84 |
| Ce | 15 | | 27 | | 180 | | 111 |
| Ce | 18 | | 30 | | 167 | | 120 |
| Ce | 20 | 18 | 29 | 90 | 145 | 161 | 85 |
| Ce | | | 35 | | | | |
| Ce | 25 | | | | | | |
| Ce | 27 | 23 | | 85 | | | 235 |
| Ce | | 26 | | | | | |
| Ce | 33 | | | | | | |
| Ce | 33 | 29 | *41* | 88 | 124 | 141 | 94 |
| Ce | 35 | 31 | 43 | 89 | 123 | 139 | 95 |
| Ce | 34 | | | | | | |
| Ce | 35 | | | | | | |
| Ce | 36 | 29 | *44* | 81 | 122 | 152 | 99 |
| Ce | 39 | 35 | 46 | 90 | 118 | 131 | 96 |
| Ce | 38 | 37 | *50* | 97 | 132 | 135 | 87 |
| Ce | 40 | 36 | *56* | 90 | 140 | 156 | 87 |
| Ce | 41 | 35 | 56 | 85 | 137 | 160 | 90 |
| Ce | 41 | 40 | 57 | 98 | 139 | 143 | 85 |
| Ce | 43 | 41 | 55 | 95 | 128 | 134 | 90 |
| Ce | 43 | 41 | 57 | 95 | 133 | 139 | 88 |
| Ce | 43 | 40 | 60 | 93 | 140 | 150 | 86 |
| Ce | 43 | 44 | *67* | 102 | 156 | 152 | 77 |
| Ce | 43 | 44 | 67 | 102 | 156 | 152 | 77 |
| D | 42 | 45 | 68 | 107 | 162 | 151 | 74 |
| D | 48 | | 62 | | 129 | | |
| D | 47 | 51 | 59 | 109 | 126 | 116 | 85 |
| D | 47 | 52 | 60 | 111 | 128 | 115 | 84 |
| D | 45 | 49 | 62 | 109 | 138 | 127 | 81 |
| D | 43 | 49 | 61 | 114 | 142 | 124 | 78 |
| Ca | 32 | 45 | 57 | 141 | 178 | 127 | 63 |
| Ca | 33 | 46 | 60 | 139 | 182 | 130 | 62 |
| Ca | 34 | | 62 | | 182 | | |
| Ca | 35 | | | | | | |

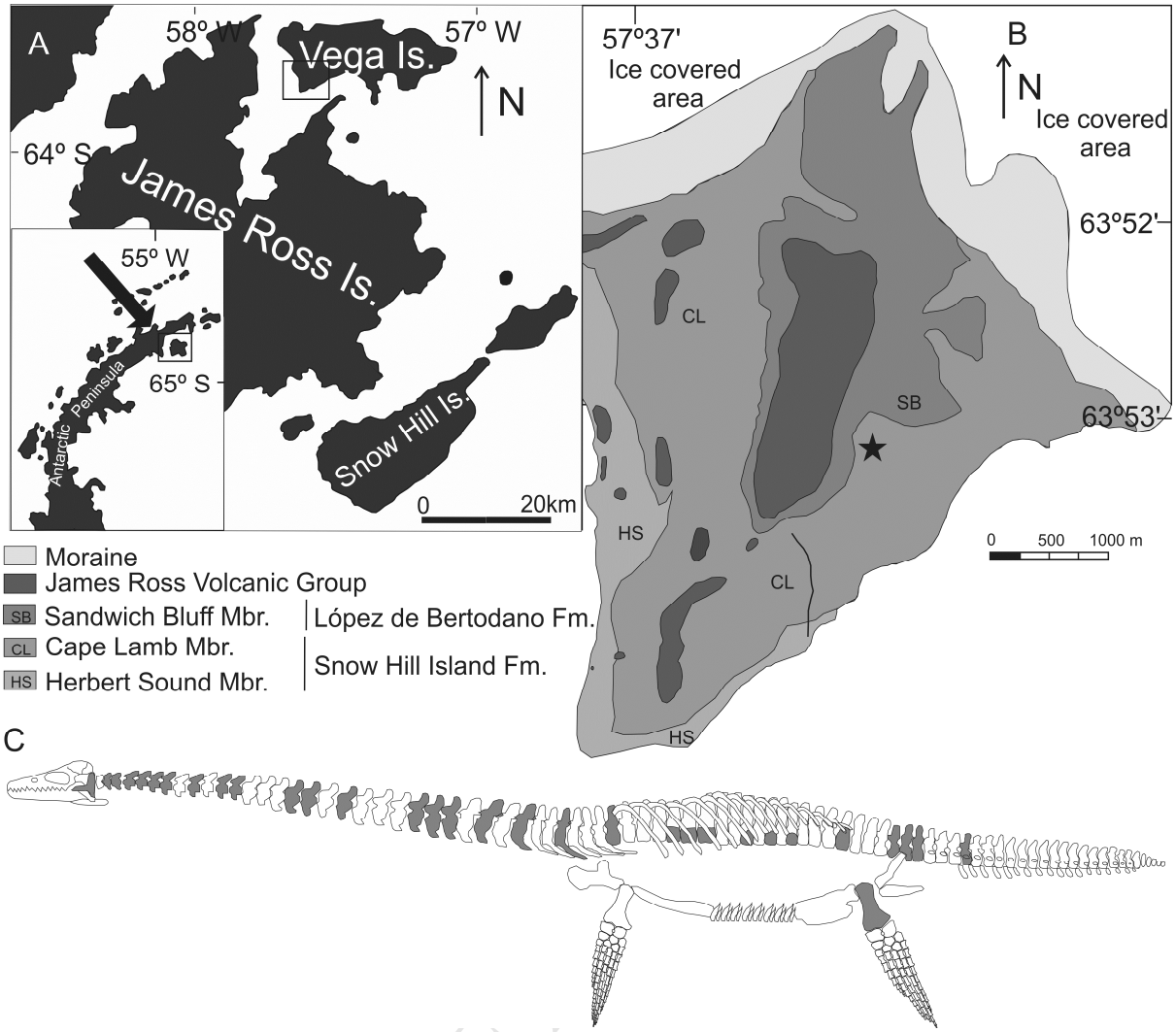
A
58° W
57° W
Vega Is.
N
64° S
James Ross Is.
55° W
65° S
Antarctic Peninsula
Snow Hill Is.
0 20km
B
57°37'
Ice covered area
N
Ice covered area
63°52'
63°53'
CL
SB
HS
CL
HS
0 500 1000 m
Moraine
James Ross Volcanic Group
SB Sandwich Bluff Mbr.
CL Cape Lamb Mbr.
HS Herbert Sound Mbr.
López de Bertodano Fm.
Snow Hill Island Fm.
C

ACCEPTED

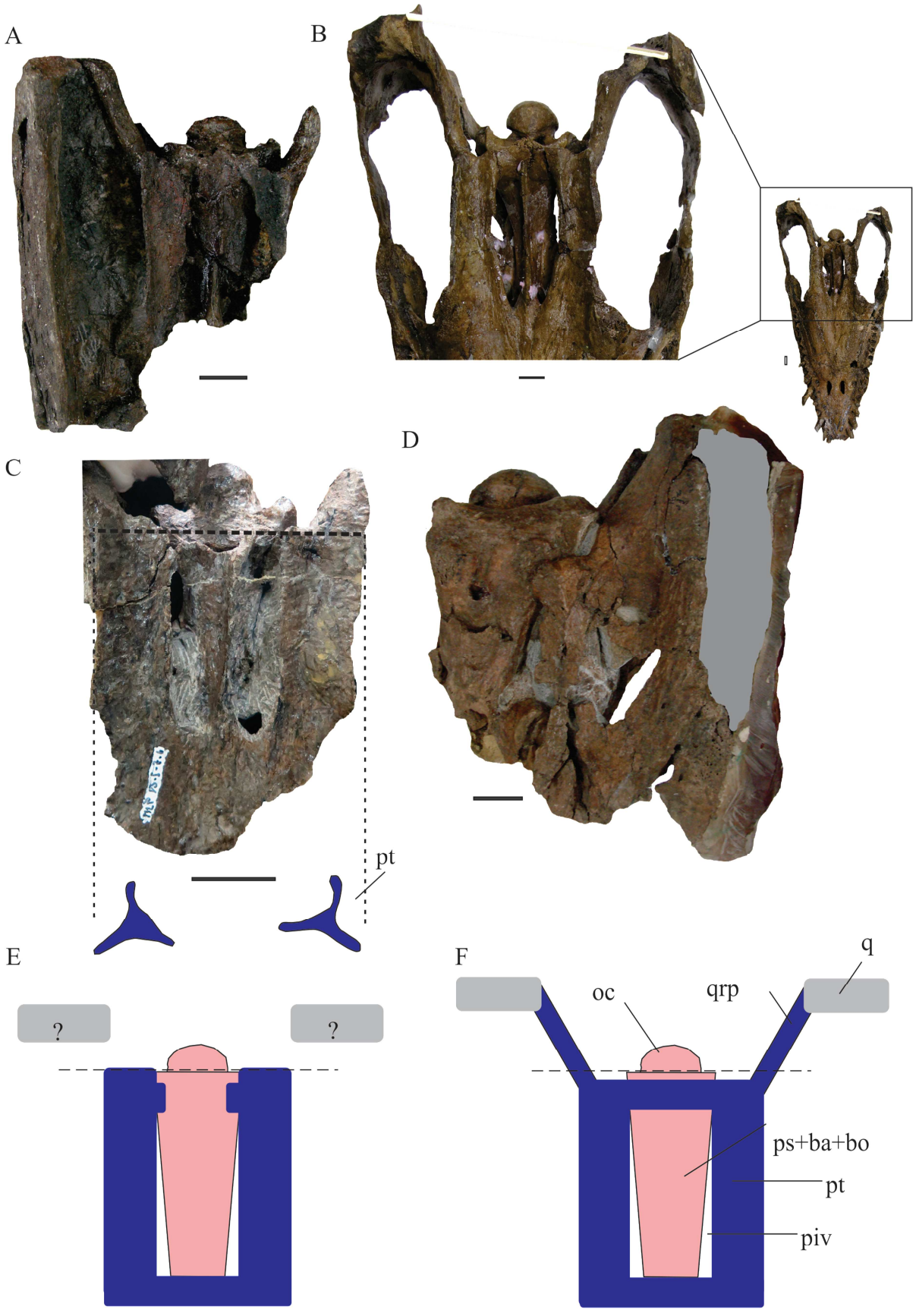
A
B
C
D
pt
E
?
?
F
q
oc
qrp
ps+ba+bo
pt
piv

A

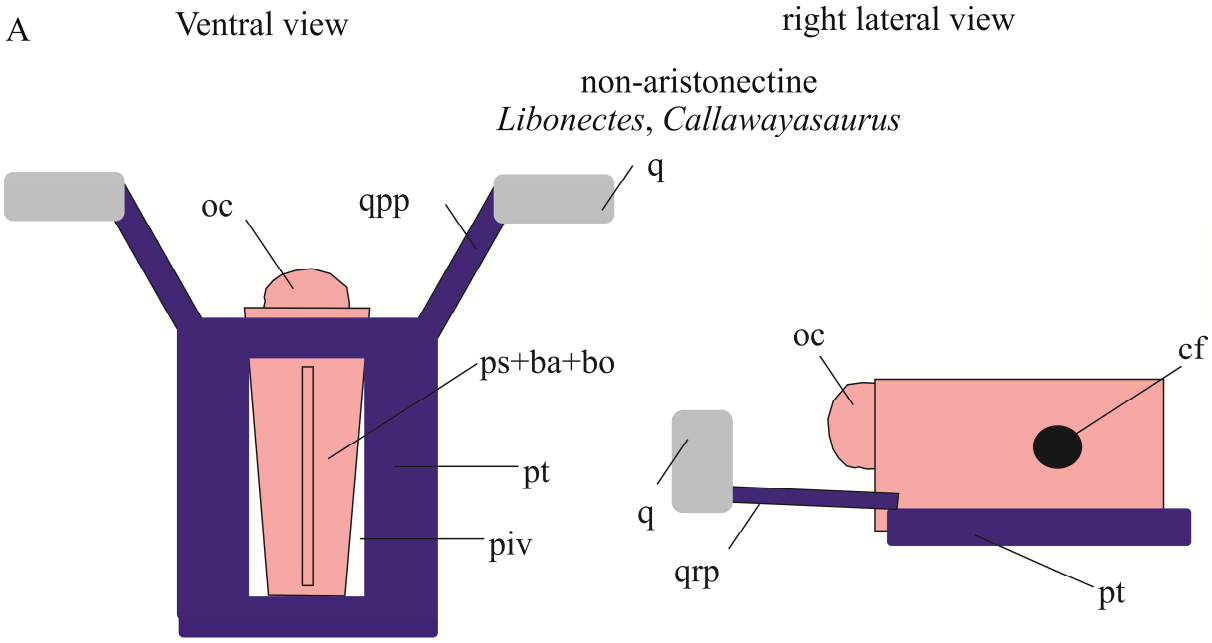
Ventral view
right lateral view
non-aristonectine
*Libonectes*, *Callawayasaurus*
oc
qpp
q
ps+ba+bo
pt
piv
oc
cf
q
qrp
pt

B

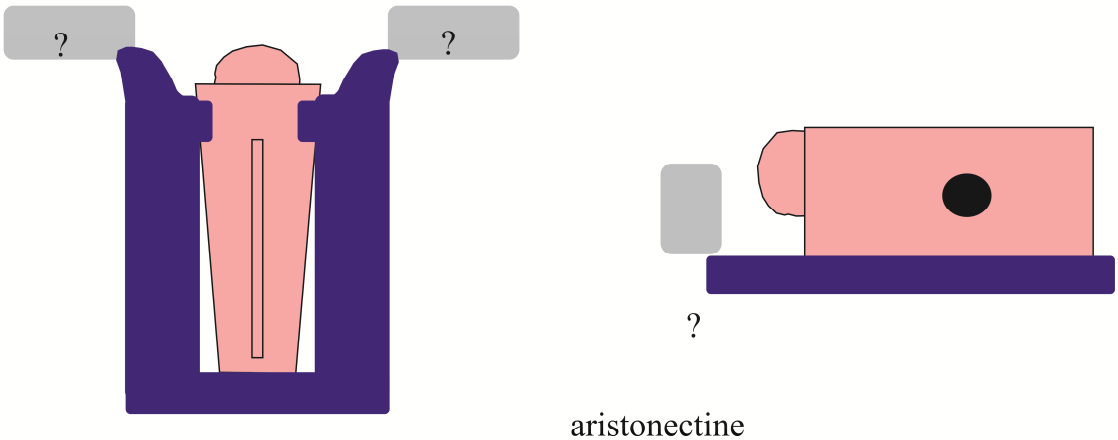
non-aristonectine MLP 15-I-7-6
?
?
?

C

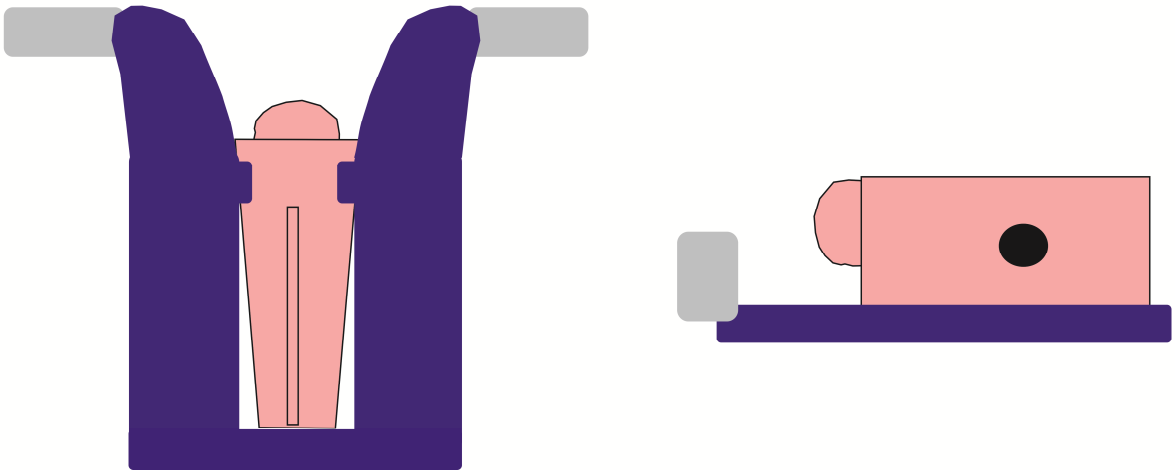
aristonectine
*Aristonectes; Alexandronectes, Kaiwhekea*

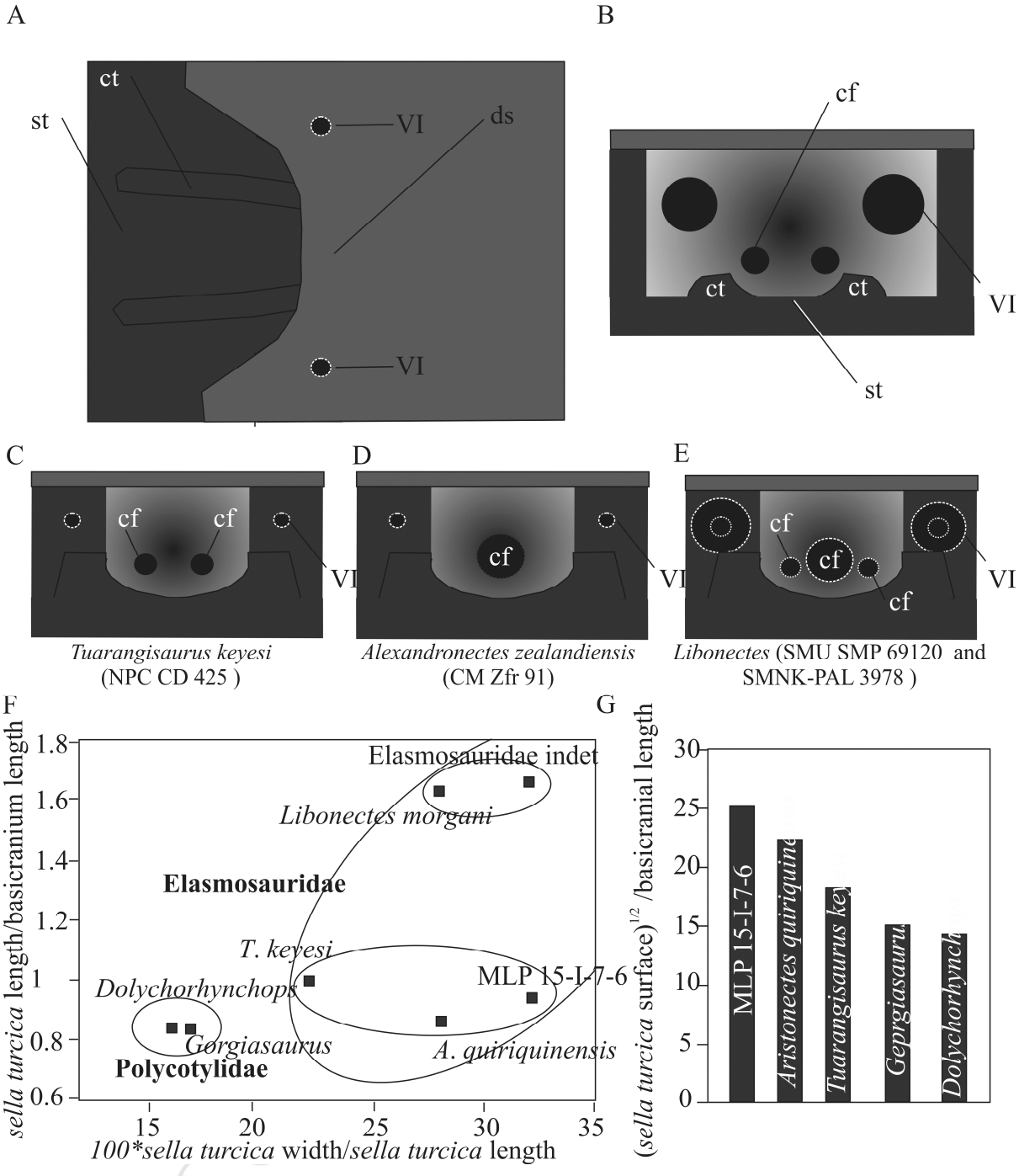
A
ct
st
VI
ds
VI
B
cf
ct
ct
VI
st
C
cf
cf
VI
D
cf
VI
E
cf
cf
cf
VI
Tuarangisaurus keyesi
(NPC CD 425 )
Alexandronectes zealandiensis
(CM Zfr 91)
Libonectes (SMU SMP 69120 and
SMNK-PAL 3978 )
F
sella turcica length/basicranium length
1.8
1.6
1.4
1.2
1
0.8
0.6
Elasmosauridae indet
Libonectes morgani
Elasmosauridae
T. keyesi
Dolychorhynchops
MLP 15-I-7-6
Gorgiasaurus
A. quiriquinensis
Polycotylidae
15
20
25
30
35
100*sella turcica width/sella turcica length
G
(sella turcica surface)1/2 /basicranial length
30
25
20
15
10
5
0
MLP 15-I-7-6
Aristonectes quiriquine
Tuarangisaurus ke
Geprgiasauru
Dolychorhynch

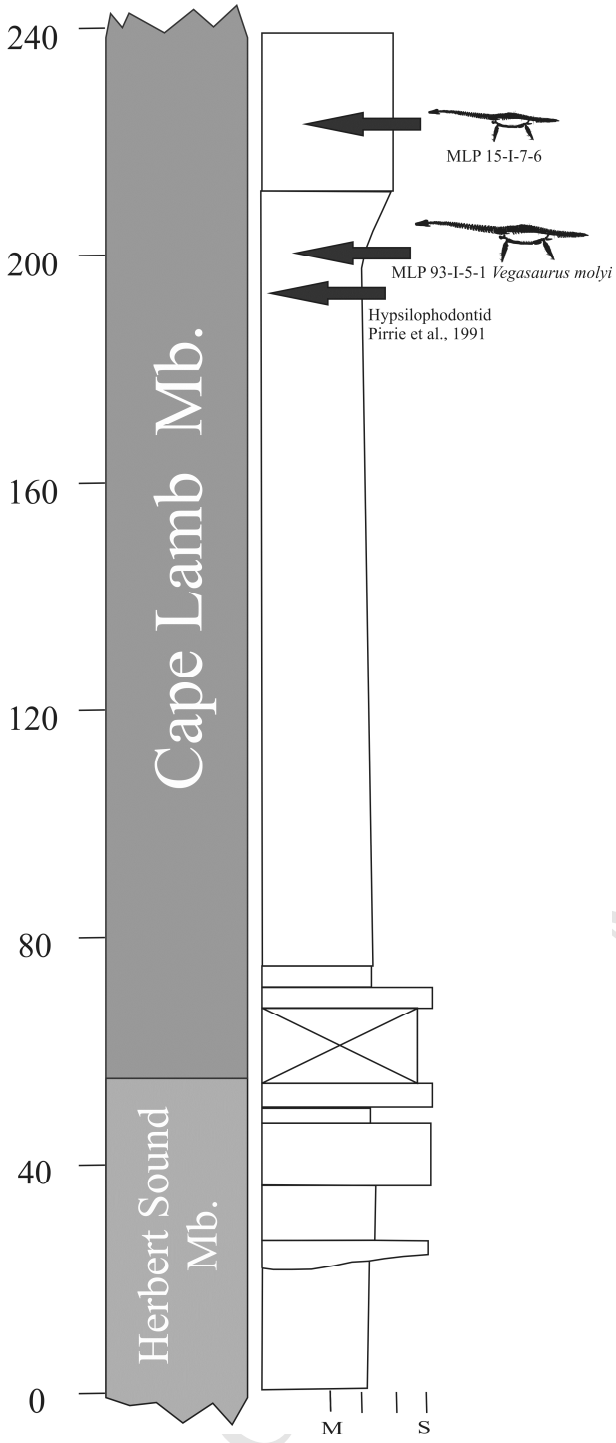
240
200
160
120
80
40
0
Cape Lamb Mb.
Herbert Sound Mb.
MLP 15-I-7-6
MLP 93-I-5-1 Vegasaurus molyi
Hypsilophodontid
Pirrie et al., 1991
M
S

MANUSCRIPT

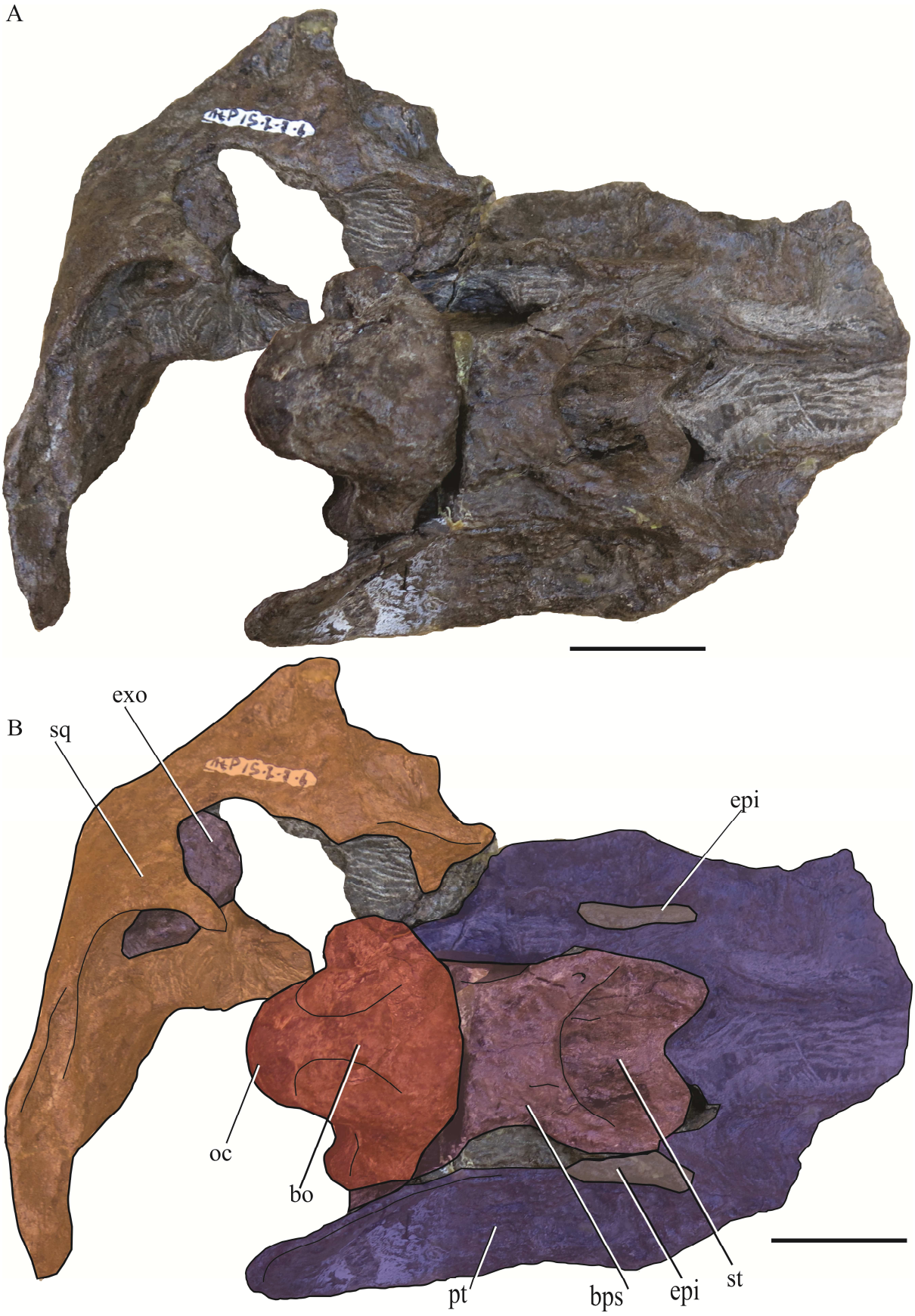
A
B
exo
sq
epi
oc
bo
pt
bps
epi
st

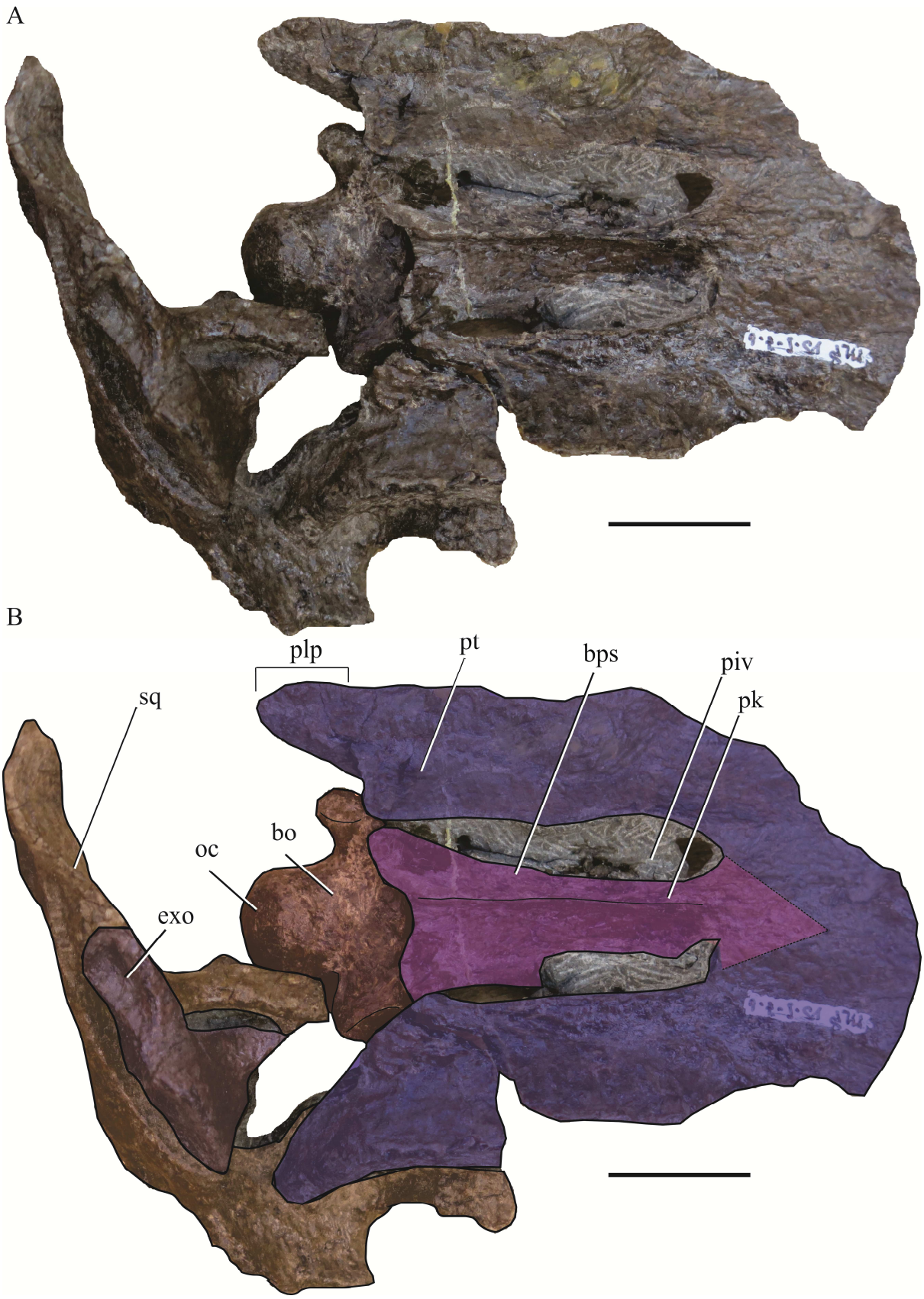
A
B
plp
pt
bps
piv
pk
sq
bo
oc
exo

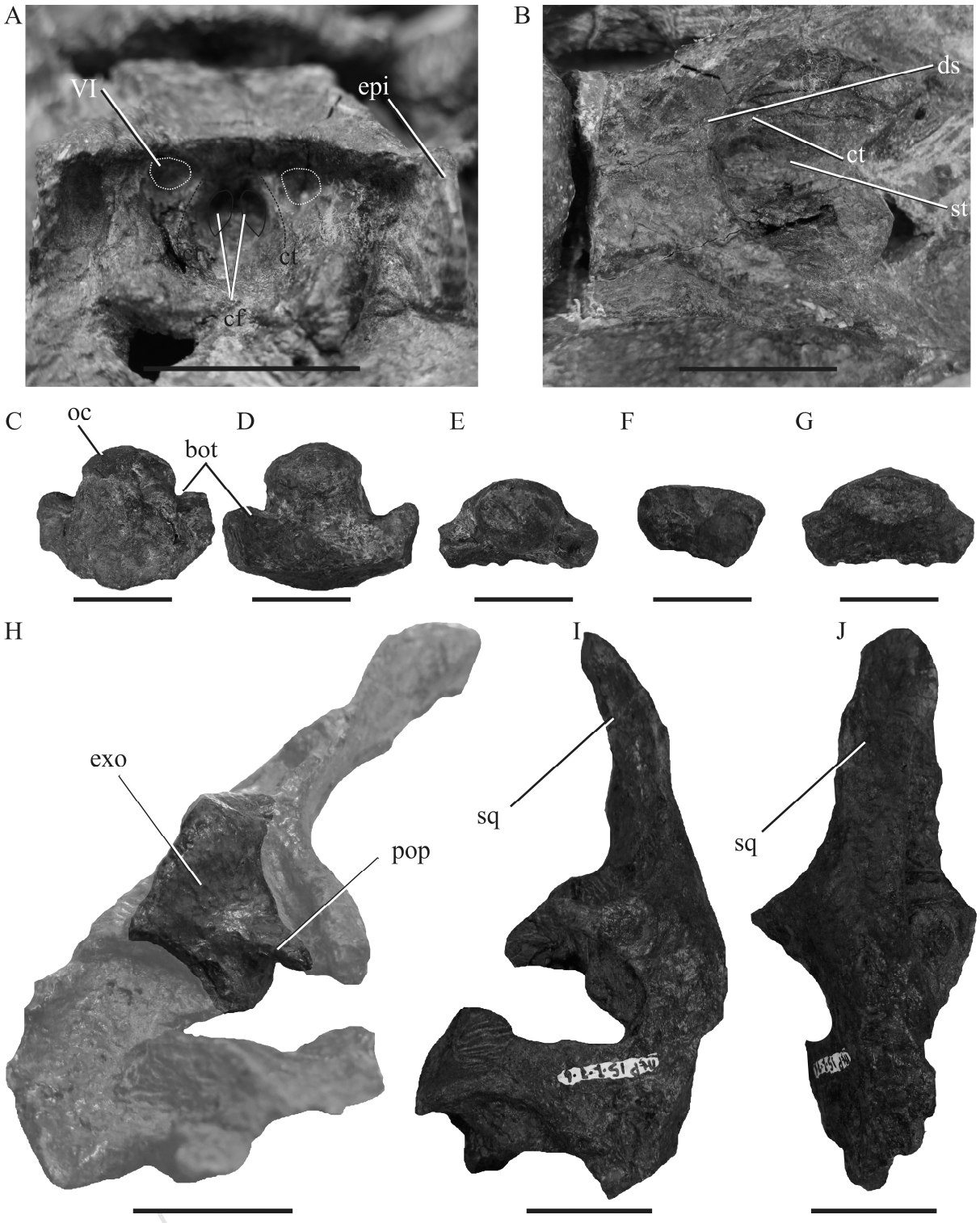
A
VI
epi
ct
cf
B
ds
ct
st
C
oc
bot
D
E
F
G
H
exo
pop
I
sq
J
sq

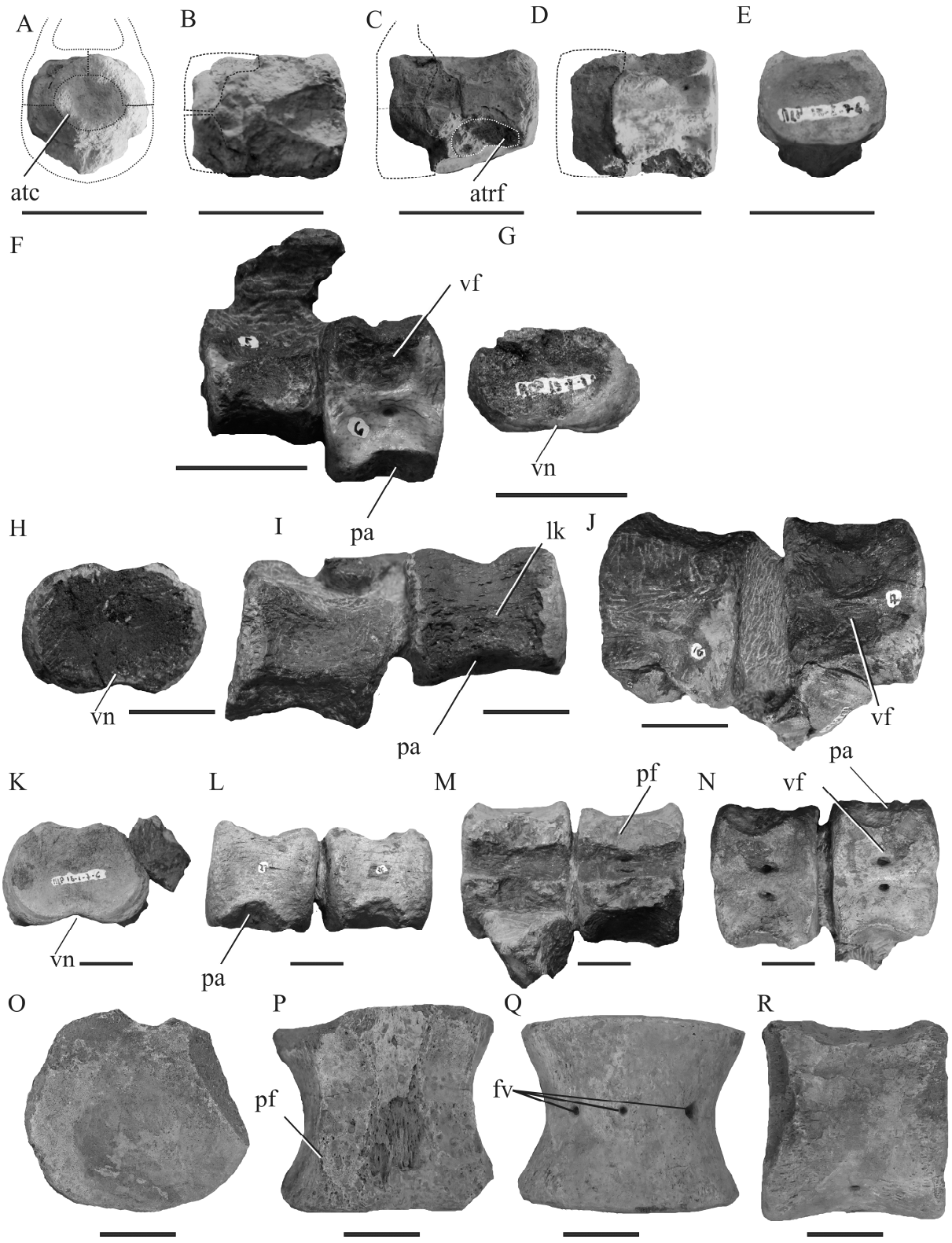
A
B
C
D
E
atc
atrf
F
G
vf
vn
pa
H
I
J
lk
vn
pa
vf
K
L
M
N
pf
vf
pa
vn
pa
O
P
Q
R
pf
fv

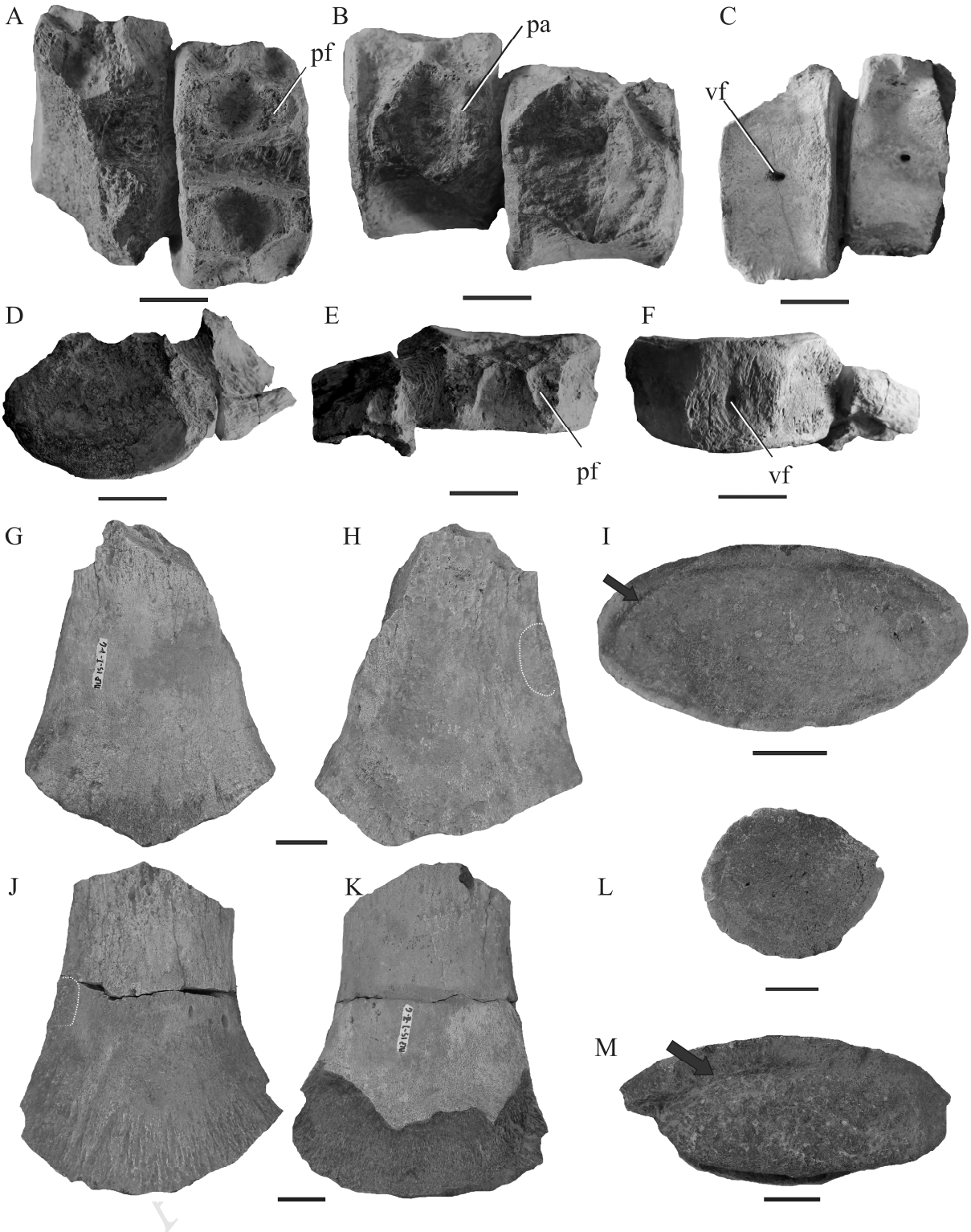
A
pf
B
pa
C
vf
D
E
pf
F
vf
G
H
I
J
K
L
M

ACCEPTED MANUSCRIPT

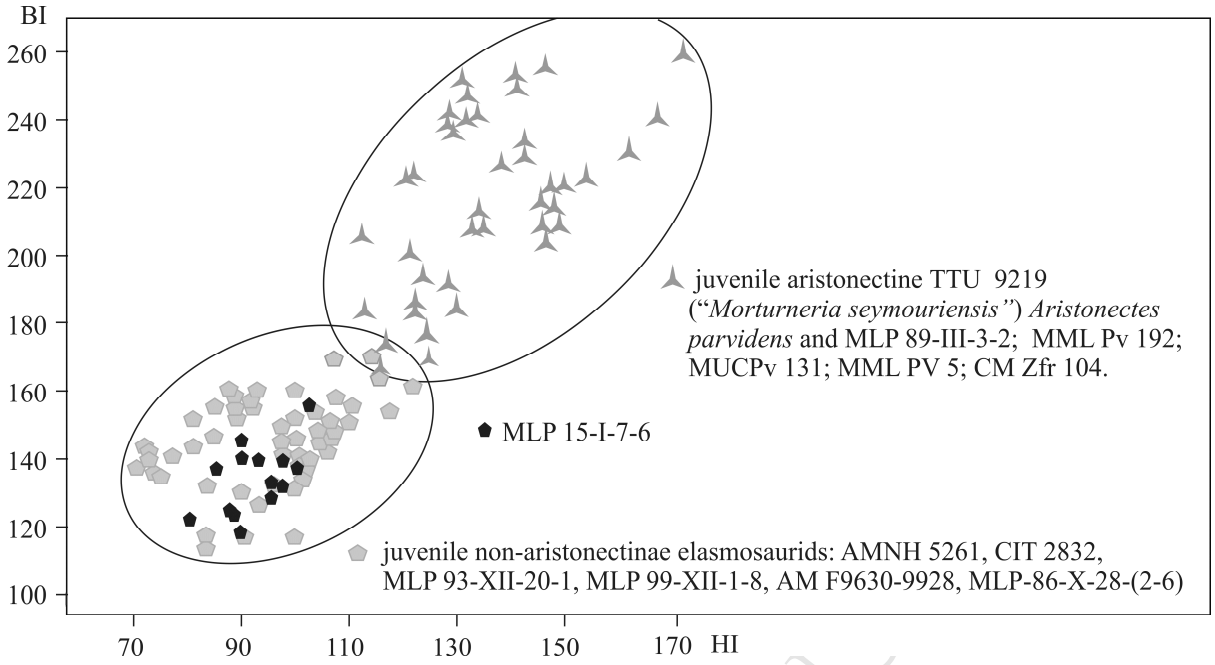


ACCEPTED MANUSCRIPT

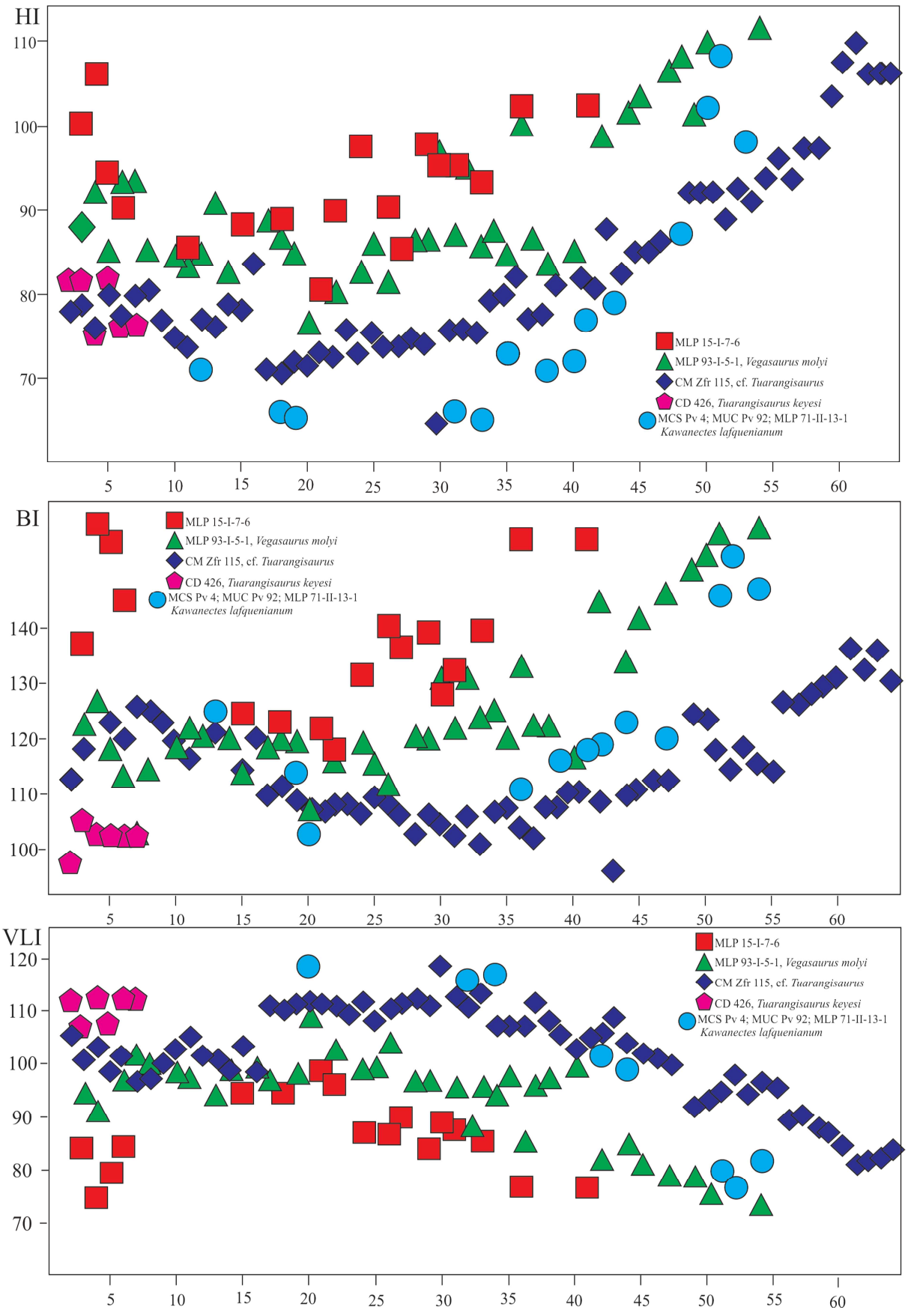
HI
110
100
90
80
70
5
10
15
20
25
30
35
40
45
50
55
60
MLP 15-I-7-6
MLP 93-I-5-1, Vegasaurus molyi
CM Zfr 115, cf. Tuarangisaurus
CD 426, Tuarangisaurus keyesi
MCS Pv 4; MUC Pv 92; MLP 71-II-13-1
Kawanectes lafquenianum
BI
140
130
120
110
100
VLI
120
110
100
90
80
70